doi:10.1038/nature09626

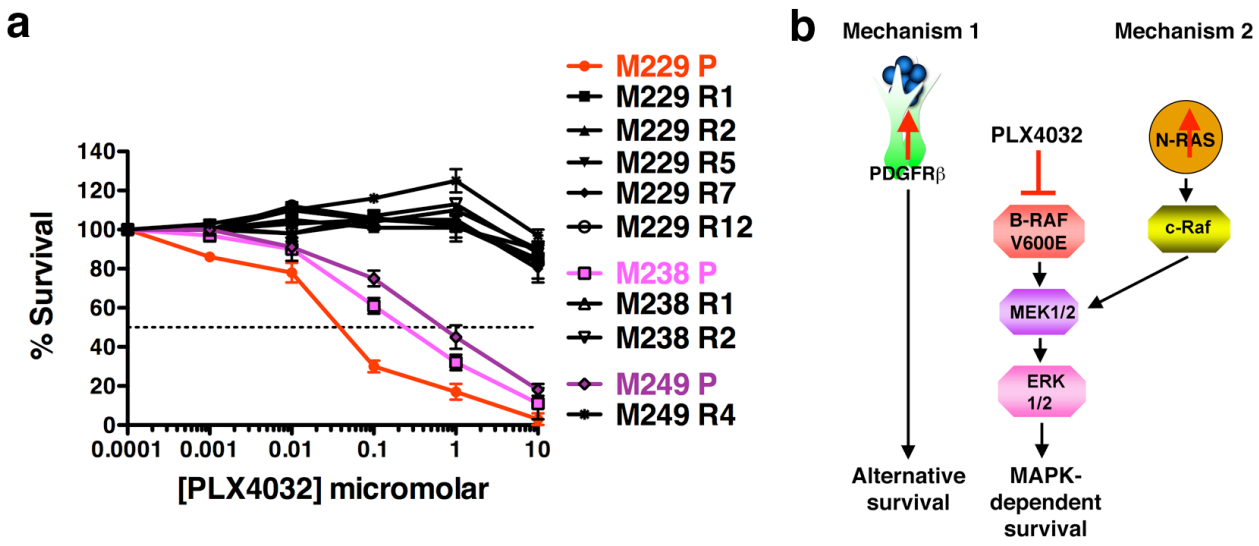

Suppl. Figure 1. *In vitro* isogenic models of PLX4032 acquired resistance and a model of acquired resistance mechanisms to PLX4032. **a,** Survival curves for parental melanoma cell lines and their isogenic PLX4032-resistant sub-lines. Cells were treated with the indicated [PLX4032] for 72 h. Data represent percent surviving cells relative to DMSO-treated controls (mean ± SEM, n = 5). The dashed line corresponds to 50% cell killing. **b,** ^{V600E}B-RAF from PLX4032-resistant melanomas lacks secondary mutations and remains sensitive to PLX4032 *in vitro*. Instead, melanomas acquiring resistance to PLX4032 utilize distinct escape pathways involving RTK-mediated alternative survival signaling or MAPK reactivation.

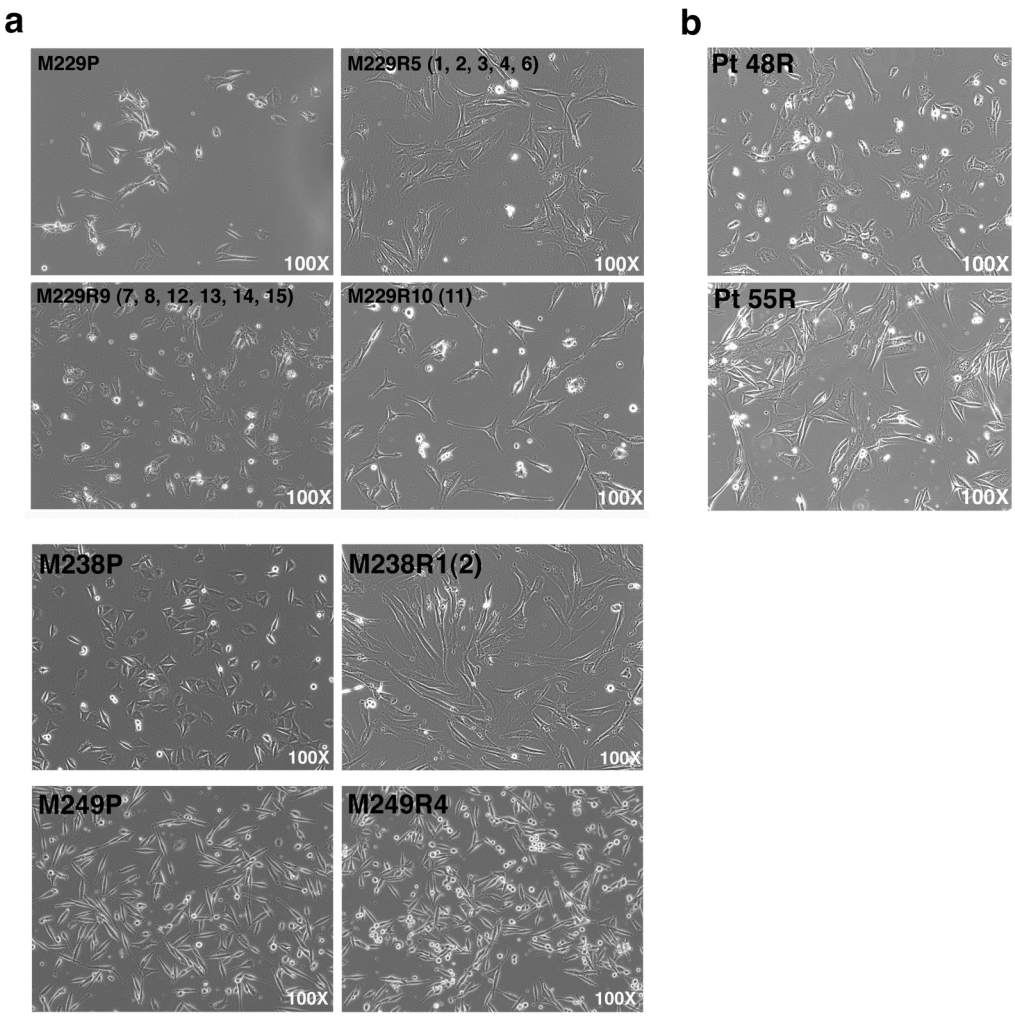

Suppl. Figure 2. Cellular morphologies of isogenic cell line models and melanoma cultures derived from PLX4032-resistant tumors. a, ^{V600E}B-RAF-positive M229, M238 and M249 parental melanoma cell lines and their PLX4032-resistant sub-lines derived *in vitro* (100X). M229 R and M238 R sub-lines tend to be flatter, larger cells, and more fibroblast-like compared with their parental cell lines, M229 and M238. On the other hand, M249 P and R4 appear indistinguishable except for a greater number of detached, trypan blue-excluding, viable cells in the latter. **b,** Short-term melanoma cultures derived from two patients whose tumors relapsed on continuous oral dosing of PLX4032 (100X).

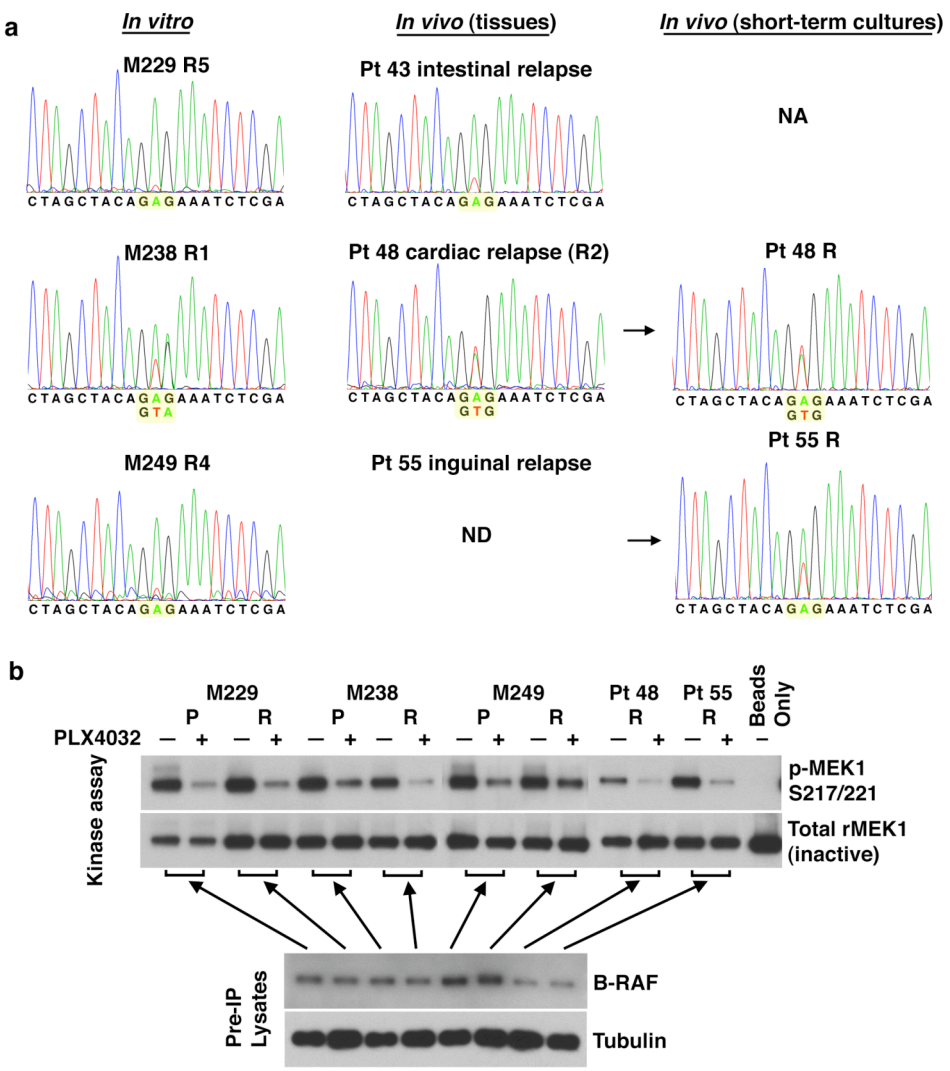

Suppl. Figure 3. B-RAF from PLX4032-resistant sub-lines, tumors and short-term cultures retains V600E mutation, lacks secondary mutation, and displays similar *in vitro* PLX4032 sensitivity as B-RAF from parental cell lines. a, Codons encoding glutamic acid at amino acid position 600 highlighted in yellow. NA, not available; ND, not displayed. **b,** Cells were lysed and B-RAF was immunoprecipitated (IP), washed and subjected to *in vitro* kinase assay. Kinase activity was determined by immunoblotting for pMEK1. Pre-IP lysates were immunoblotted for B-RAF and tubulin levels. Beads only, no B-RAF antibody added to M229 P lysate prior to kinase assay.

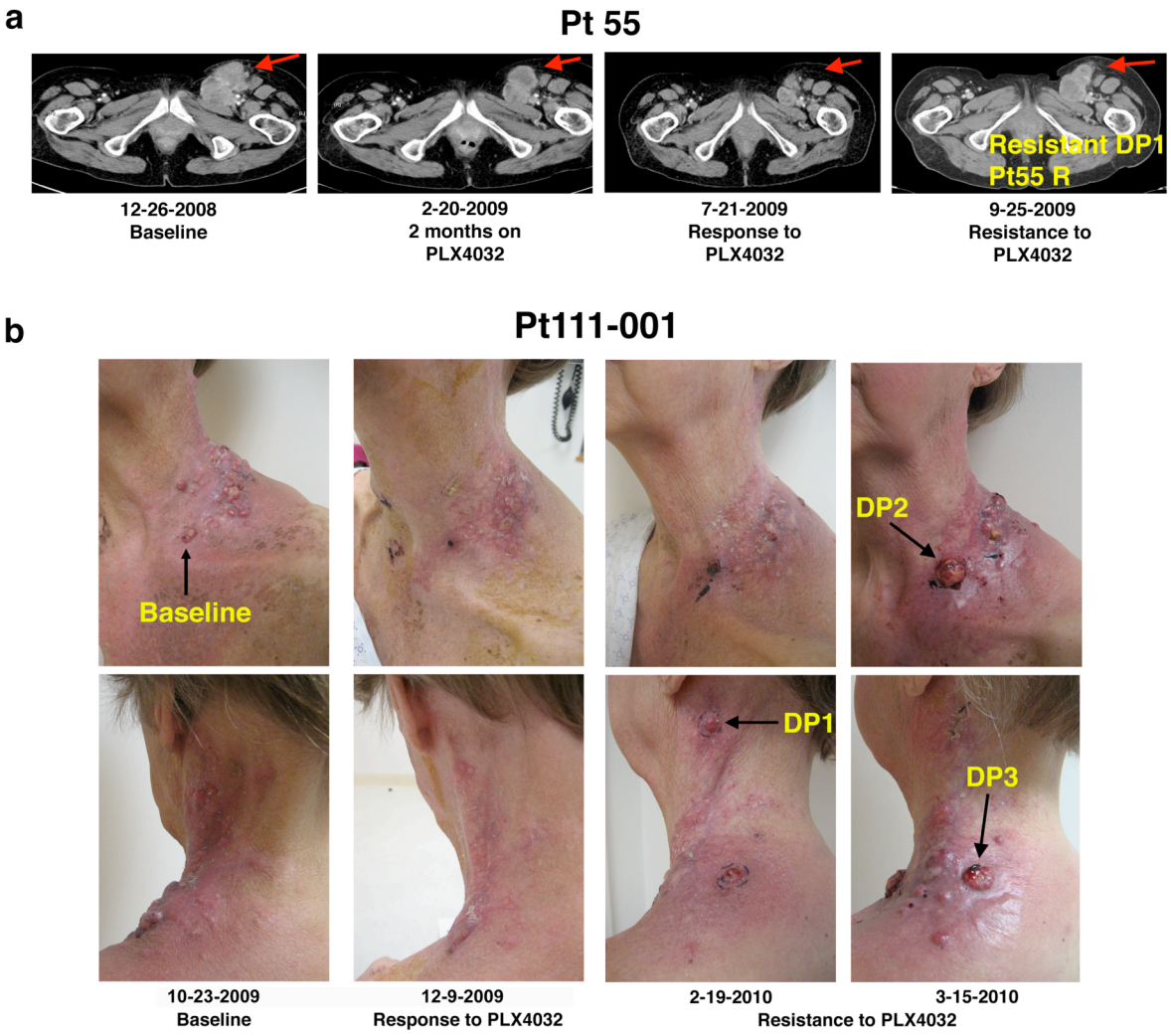

Suppl. Figure 4. Melanoma tumor response to and progression on PLX4032 treatment in two patients: examples of tissues analyzed in the present study. a, Computed tomography scans of Pt55 whose left groin melanoma tumor responded to and subsequently relapsed on continuous oral PLX4032 dosing. **b**, Clinical photographs of Pt111-001 whose cutaneous metastases responded and then acquired resistance to PLX4032. DP (Disease Progression) 2 biopsy occurred at the same site as that of the baseline biopsy.

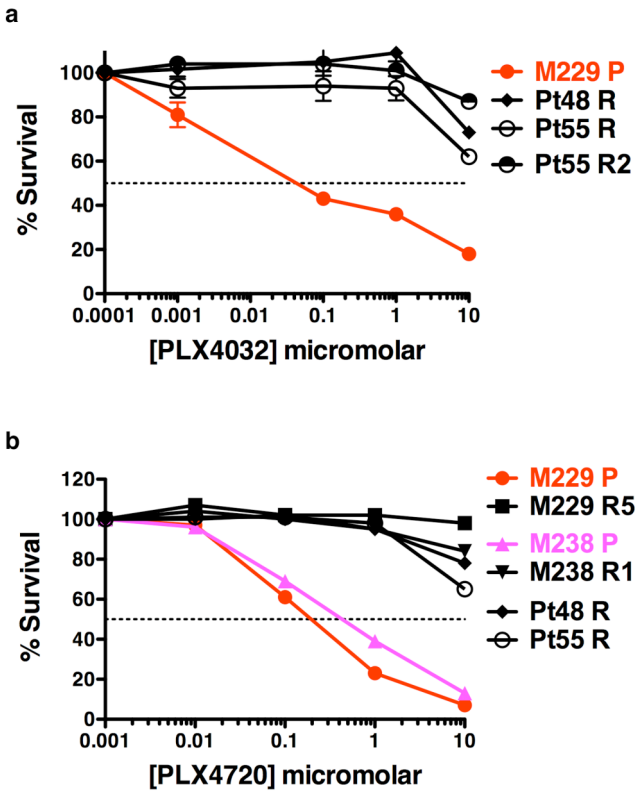

Suppl. Figure 5. Pt48 R and Pt55 R, derived from tumors in patients relapsing on PLX4032, are resistant to PLX4032 and PLX4720 *in vitro*. **a,** Survival curves for parental M229 melanoma cell line (as a control PLX4032-sensitive cell line) and short-term melanoma cultures Pt48 R, Pt55 R, and Pt55 R2. **b,** Sensitivity of Pt48 R and Pt55 R to PLX4720 is compared to that of the M229 and M238 isogenic cell line pairs. Cells were treated with the indicated [PLX4032] or [PLX4720] for 72 h. Data represent percent surviving cells relative to DMSO-treated controls (mean ± SEM, n = 5). The dashed line corresponds to 50% cell killing.

a

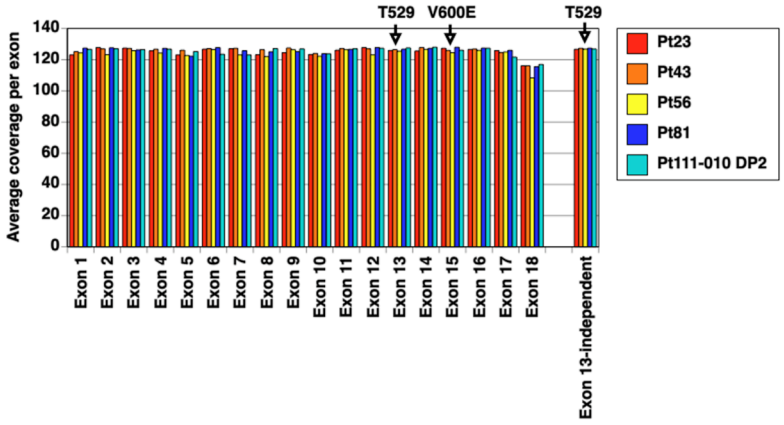
T529
V600E
T529
Average coverage per exon
140
120
100
80
60
40
20
0
Exon 1
Exon 2
Exon 3
Exon 4
Exon 5
Exon 6
Exon 7
Exon 8
Exon 9
Exon 10
Exon 11
Exon 12
Exon 13
Exon 14
Exon 15
Exon 16
Exon 17
Exon 18
Exon 13-independent
Pt23
Pt43
Pt56
Pt81
Pt111-010 DP2

b

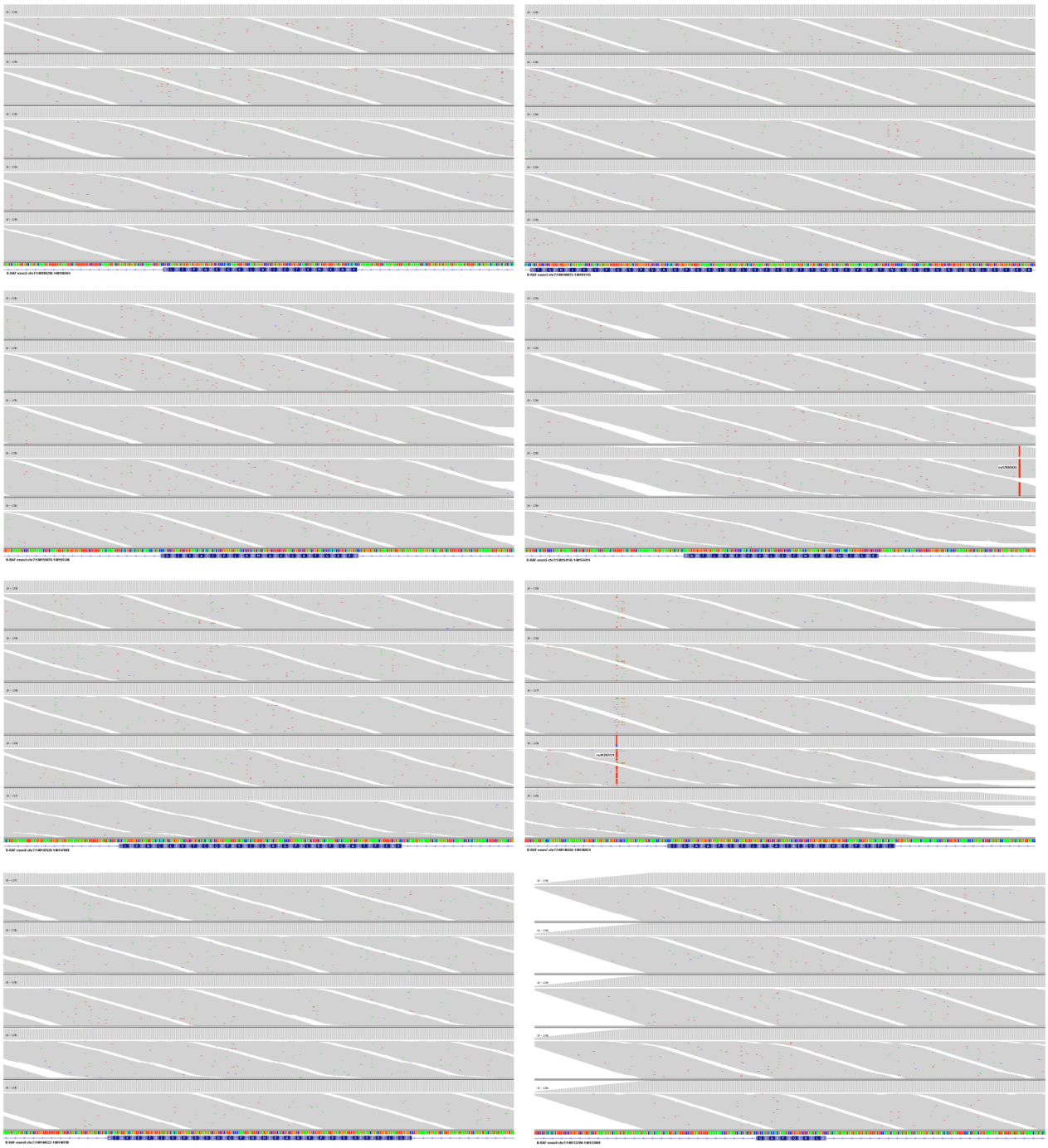

b continued

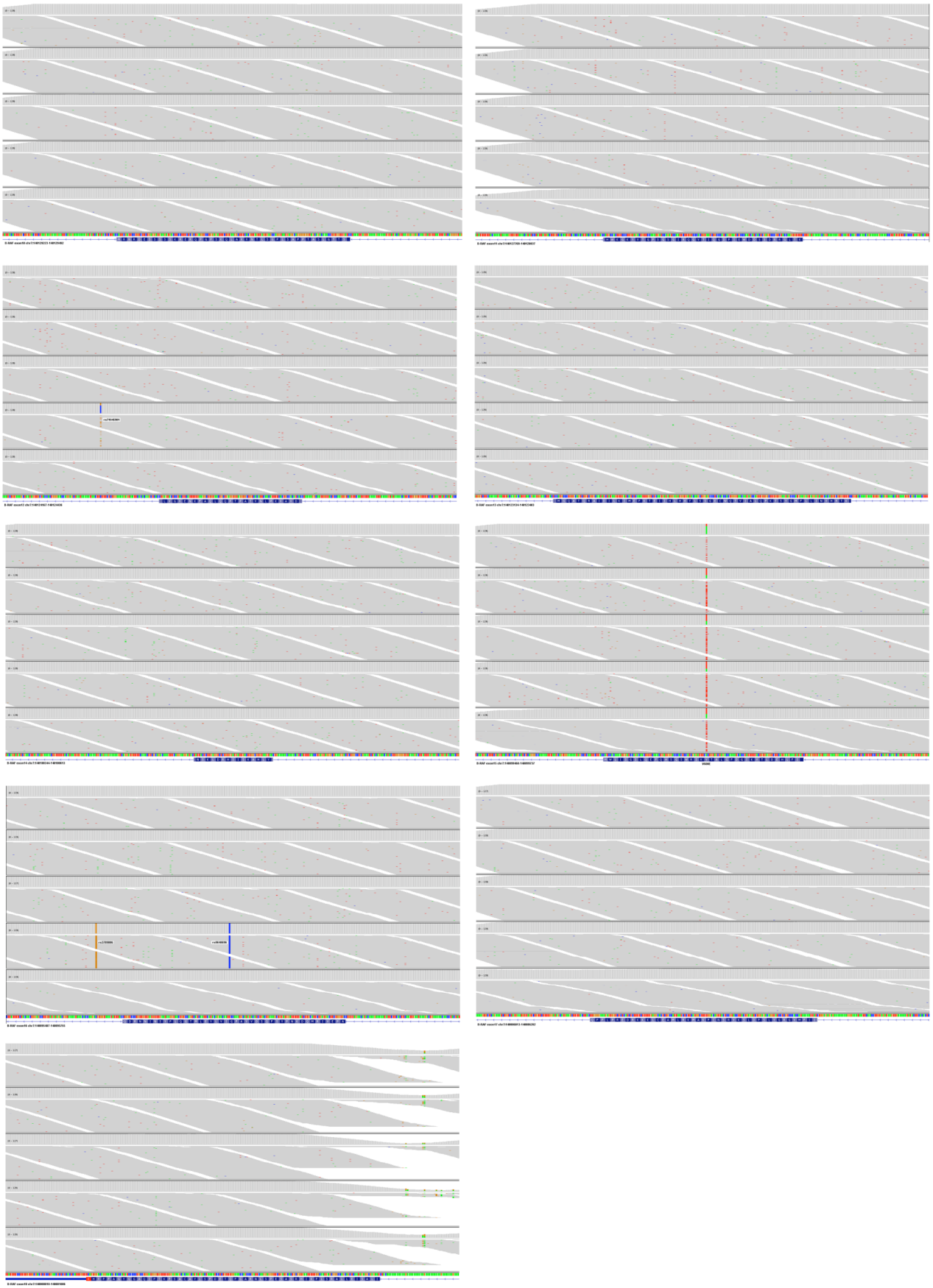

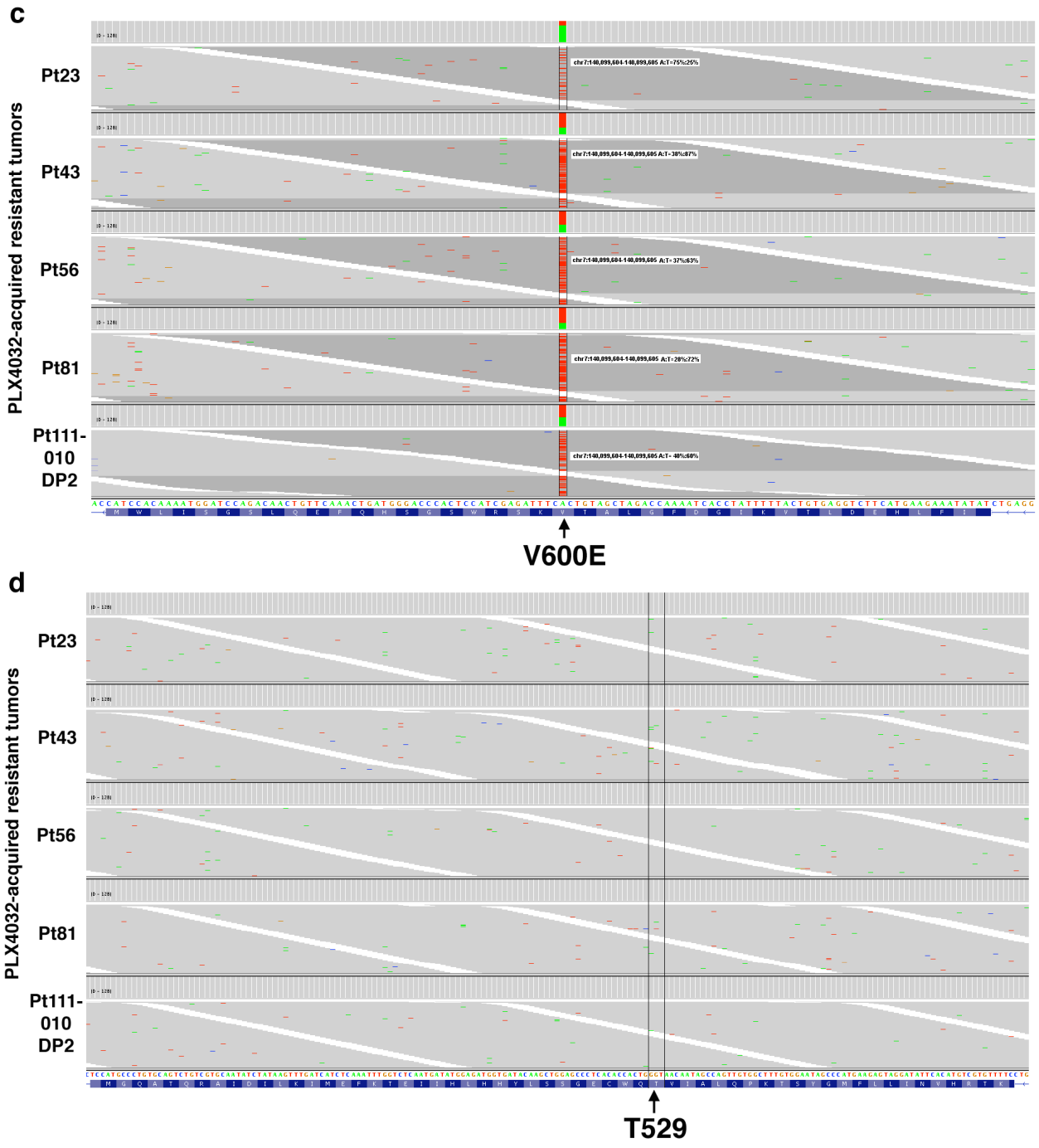

Suppl. Figure 6. Ultradeep sequencing of melanoma tumors with acquired resistance to PLX4032 shows a lack of secondary mutations in ^{V600E}*B-RAF*.

a, Average *B-RAF* exon coverage and independent exon 13 coverage achieved for five tumors from five patients. Amino acid positions of the gatekeeper residue T529 and the

activating mutation V600E shown by arrows. **b,** IGV (Integrative Genomics Viewer) plots of *B-RAF* exon 2-18 (in order left to right for each row). For small exons, the intervals were extended to achieve equivalent scale. Known SNPs are annoted in exons 5, 7, 12 and 16. **c,** IGV plot of *B-RAF* exon15 (chr7:140,099,542-140,099,668) showing the V600E mutation. The ratio of the reference allele (A: green) and the non-reference allele (T: red) is shown for each sample. **d,** IGV plot of *B-RAF* exon13 (chr7:140,123,180-140,123,360) showing the T529 position (between the two black lines) showing no non-reference allele counts above background noise level. For each sample, the top panel represents the coverage for each nucleotide (number on the left showing the coverage range for each sample). If a variant were called for a certain position, the bar would be multi-colored to represent the ratio of the alleles called. The bottom panel represents the stack of sequence reads sorted by the start position. Non-reference variant nucleotides are shown in color and embedded in individual sequence reads (reference nucleotides, grey). The non-reference alleles are shown in color (red, T; blue, C; green, A; brown, G); lighter shades of color represent low base quality (< Phred score 30) non-reference alleles. Reference nucleotides (bottom of each set of plots) shown in color (same color-coding) right above amino acid sequence (blue row, bottom).

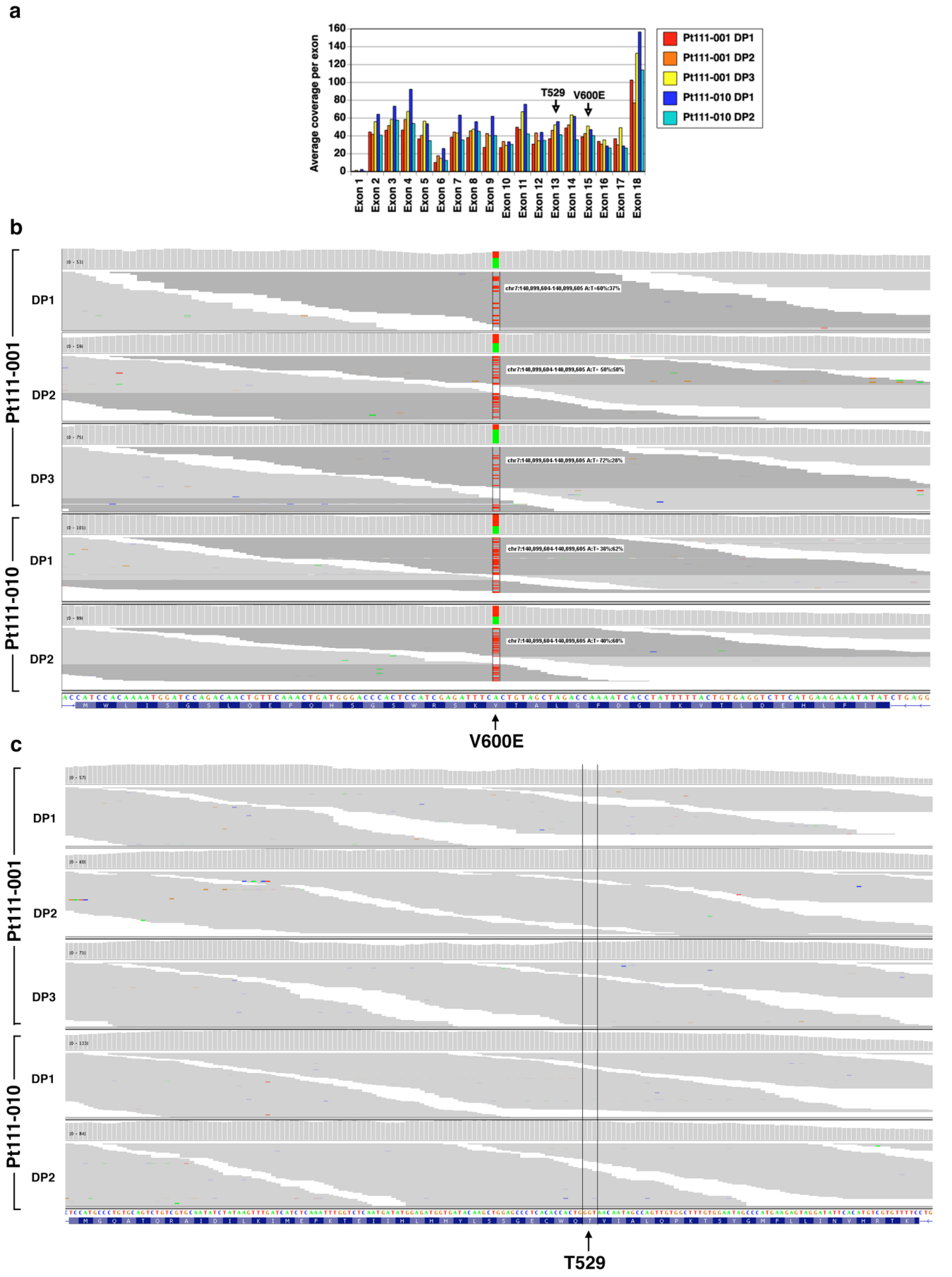
a
Average coverage per exon
160
140
120
100
80
60
40
20
0
T529
V600E
Pt111-001 DP1
Pt111-001 DP2
Pt111-001 DP3
Pt111-010 DP1
Pt111-010 DP2
Exon 1
Exon 2
Exon 3
Exon 4
Exon 5
Exon 6
Exon 7
Exon 8
Exon 9
Exon 10
Exon 11
Exon 12
Exon 13
Exon 14
Exon 15
Exon 16
Exon 17
Exon 18
b
Pt111-001
Pt111-010
DP1
DP2
DP3
DP1
DP2
V600E
c
Pt111-001
Pt111-010
DP1
DP2
DP3
DP1
DP2
T529

Suppl. Figure 7. Deep sequencing of melanoma tumors with acquired resistance to PLX4032 shows a lack of secondary mutations in ^{V600E}*B-RAF*. **a**, Average *B-RAF* exon coverage achieved for five tumors from two patients (Pt111-001 samples shown in Supplementary Fig. 4b). Amino acid positions of the gatekeeper residue T529 and the activating mutation V600E are shown by arrows. **b**, IGV plot (chr7:140,099,542-140,099,668) showing heterozygous ^{V600E}*B-RAF* alleles in all samples. The levels of nucleotide coverage at position 140,099,605 (reference A; consensus read A/T) for Pt111-001 (DP1, DP2, DP3) and Pt111-010 (DP1, DP2) are as follows: 43, 54, 69, 62 and 52. The ratio of the reference allele (A: green) and the non-reference allele (T: red) is shown for each sample. **c**, IGV plot (chr7:140,123,180-140,123,360) showing lack of non-reference variants at the T529 gatekeeper threonine codon. The levels of nucleotide coverage at positions 140,123,288 (reference nucleotide G), 140,123,289 (reference G), and 140,123,290 (reference T) are as follows: 41, 39, 39 (Pt111-001 DP1); 55, 55, 56 (Pt111-001 DP2); 59, 60, 60 (Pt111-001 DP3); 63, 63, 61 (Pt111-010 DP1); and 46, 46, 44 (Pt111-010 DP2). For each sample, the top panel represents the coverage for each nucleotide (number on the left showing the coverage range for each sample). If a variant were called for a certain position, the bar would be multi-colored to represent the ratio of the alleles called. The bottom panel represents the stack of sequence reads sorted by the start position. Non-reference variant nucleotides are shown in color and embedded in individual sequence reads (reference nucleotides, grey). The non-reference alleles are shown in color (red, T; blue, C; green, A; brown, G); lighter shades of color represent low base quality (< Phred score 30) non-reference

alleles. Reference nucleotides (bottom of each set of plots) shown in color (same color-coding) right above amino acid sequence (blue row, bottom).

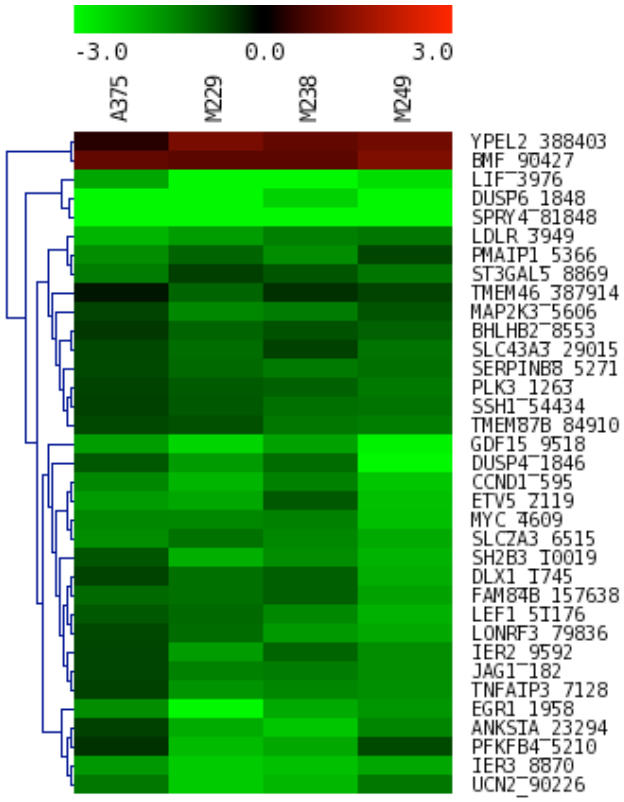

Suppl. Figure 8. PLX4032 and PLX4720 have similar effects on ^{V600E}B-RAF signature genes. Differential expression of ^{V600E}B-RAF signature genes in response to PLX4720 (A375) *vs.* PLX4032 (all others). In A375, PLX4720 induced significant (FDR < 0.05) differential expression in 31 out of 35 ^{V600E}B-RAF signature genes (88.6%) in the same direction as PLX4032 in our three parental melanoma cell lines. Differential expression of the remainder four genes in A375 in response to PLX4720 was in the same direction (but did not reach statistical significance). Heat map colors reflect $\log_2$ ratio of the PLX treatment group mean intensity over the corresponding DMSO control values. The processed data for A375 was downloaded from the Gene Expression Omnibus (GEO) database (accession GSE17089). Data from 6 h PLX4720 treatment was chosen to match our 6 h PLX4032 treatment condition.

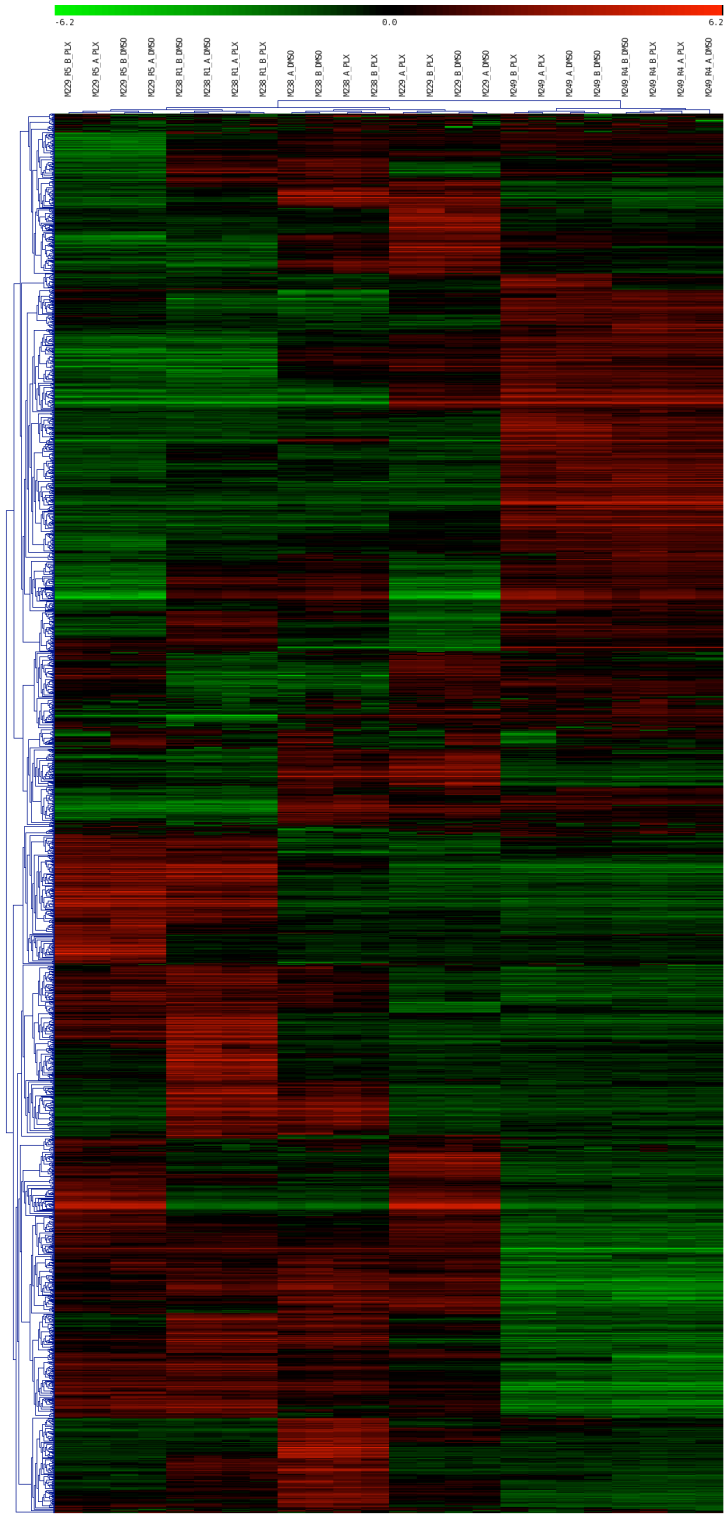

Suppl. Figure 9. Relationships among PLX4032-sensitive, parental melanoma cell lines and -resistant sub-lines based on the genomic profile of differentially

expressed genes. In a heatmap showing unsupervised clustering of these cell lines, M249 and M249R expression profiles clustered away from the rest of the cell lines, whereas M229/M238 and M229 R5/M238 R1 partitioned into closely related sub-branches. Color scale shows $\log_2$-transformed expression for each gene (row) normalized by the mean across all samples for that gene. To maximize the signal-to-noise ratio, only genes with variance two standard deviations above that of the negative control probe sets (defined by Affymetrix platform) were included. The variance for each gene was measured with $\log_2$-transformed expression across all samples.

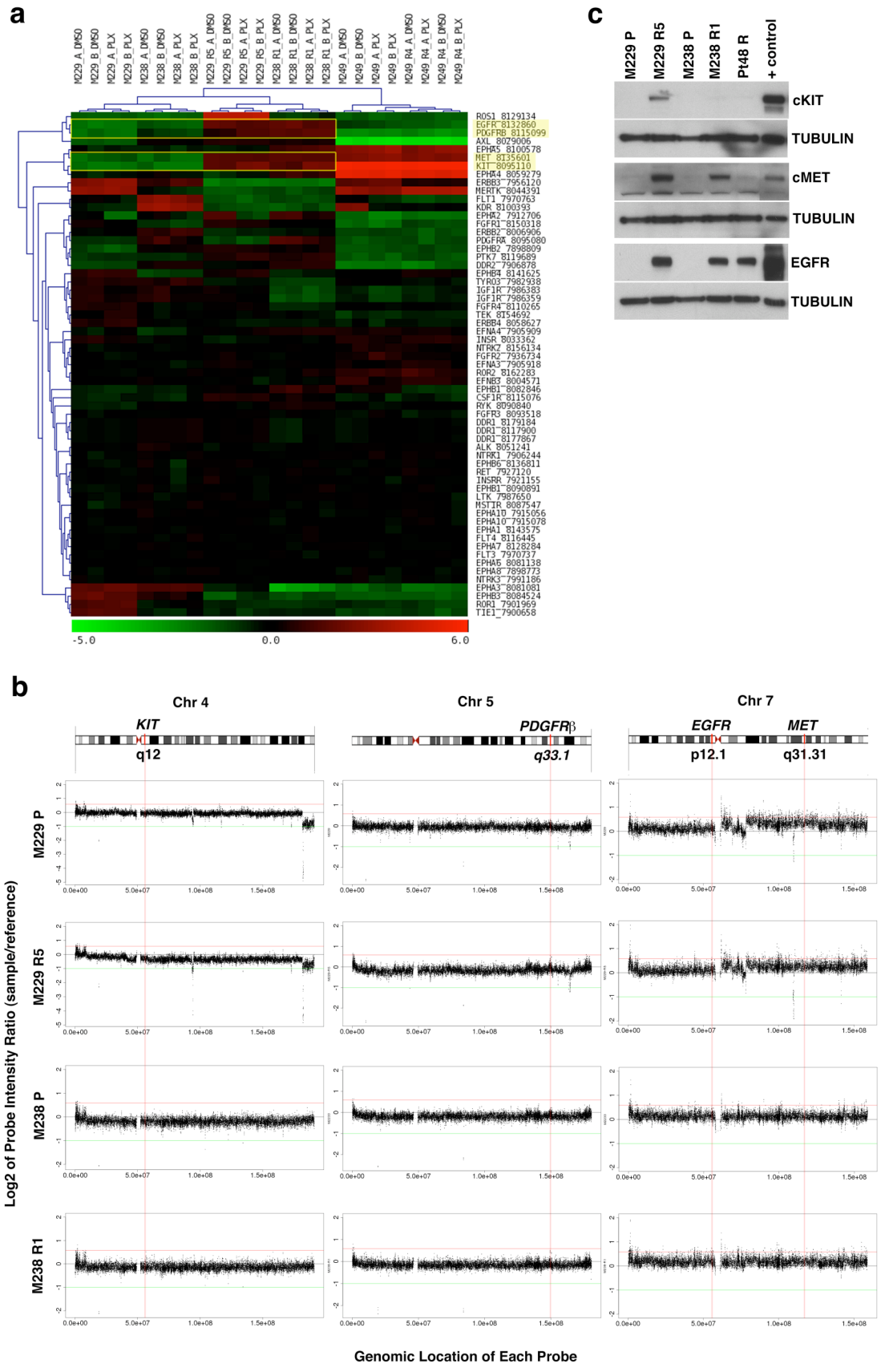
a
M229_A_DMSO
M229_B_DMSO
M229_A_PLX
M229_B_PLX
M238_A_DMSO
M238_B_DMSO
M238_A_PLX
M238_B_PLX
M229_R5_A_DMSO
M229_R5_B_DMSO
M229_R5_A_PLX
M229_R5_B_PLX
M238_R1_A_DMSO
M238_R1_B_DMSO
M238_R1_A_PLX
M238_R1_B_PLX
M249_A_DMSO
M249_B_DMSO
M249_A_PLX
M249_B_PLX
M249_R4_A_DMSO
M249_R4_A_PLX
M249_R4_B_DMSO
M249_R4_B_PLX
ROS1_8129134
EGFR_8132860
PDGFRB_8115099
AXL_8029006
EPHA5_8100578
MET_8135601
KIT_8095110
EPHB4_8059279
ERBB3_7956120
MERTK_8044391
FLT1_7970763
KDR_8100393
EPHA2_7912706
FGFR1_8150318
ERBB2_8006906
PDGFRA_8095080
EPHB2_7898809
PTK7_8119689
DDR2_7906878
EPHB4_8141625
TYRO3_7982938
IGF1R_7986383
IGF1R_7986359
FGFR4_8110265
TEK_8154692
ERBB4_8058627
EFNA4_7905909
INSR_8033362
NTRK2_8156134
FGFR2_7936734
EFNA3_7905918
ROR2_8162283
EFNB3_8004571
EPHB1_8082846
CSF1R_8115076
RYK_8090840
FGFR3_8093518
DDR1_8179184
DDR1_8117900
DDR1_8177867
ALK_8051241
NTRK1_7906244
EPHB6_8136811
RET_7927120
INSRR_7921155
EPHB1_8090891
LTK_7987650
MSTIR_8087547
EPHA10_7915056
EPHA10_7915078
EPHA1_8143575
FLT4_8116445
EPHA7_8128284
FLT3_7970737
EPHA6_8081138
EPHA8_7898773
NTRK3_7991186
EPHA3_8081081
EPHB3_8084524
ROR1_7901969
TIE1_7900658
-5.0
0.0
6.0
c
M229 P
M229 R5
M238 P
M238 R1
Pt48 R
+ control
cKIT
TUBULIN
cMET
TUBULIN
EGFR
TUBULIN
b
Chr 4
Chr 5
Chr 7
KIT
q12
PDGFRβ
q33.1
EGFR
MET
p12.1
q31.31
M229 P
M229 R5
M238 P
M238 R1
Log2 of Probe Intensity Ratio (sample/reference)
Genomic Location of Each Probe

Suppl. Figure 10. Selective over-expression of four RTKs correlates with a subset of PLX4032-resistant sub-lines but does not correlate with gDNA copy gain. a, Heatmap of RTK genes showing unsupervised hierarchical clustering of genes and samples. Color scale shows log_2-transformed expression for each gene (row) normalized by the mean of all M229 and M238 samples for each gene. Yellow boxes highlight four RTKs and their differential RNA expression patterns. **b,** PLX4032-resistant sub-lines, M229R5 and M238R1, lack gDNA copy number variations at the *KIT, PDGFRβ, EGFR and MET* loci as compared to their parental lines. Copy number variation (CNV) profiles for chromosomes four, five and seven harboring *KIT, PDGFRβ, and EGFR/MET* genes, respectively. X-axis, chromosome locations; y-axis, log_2 ratio of probe signal intensities (sample *vs*. reference). Green line, CN of 1; black, CN of 2; red, CN of 3. **c**, Relative protein levels of KIT, MET, and EGFR in PLX4032-resistant sub-lines and culture over-expressing PDGFRβ. WB positive control lysates were derived from the following: NCI-H526 (human small cell lung CA) for KIT, HCC-827 (human lung CA) for MET, and A431 (human epidermoid CA) for EGFR.

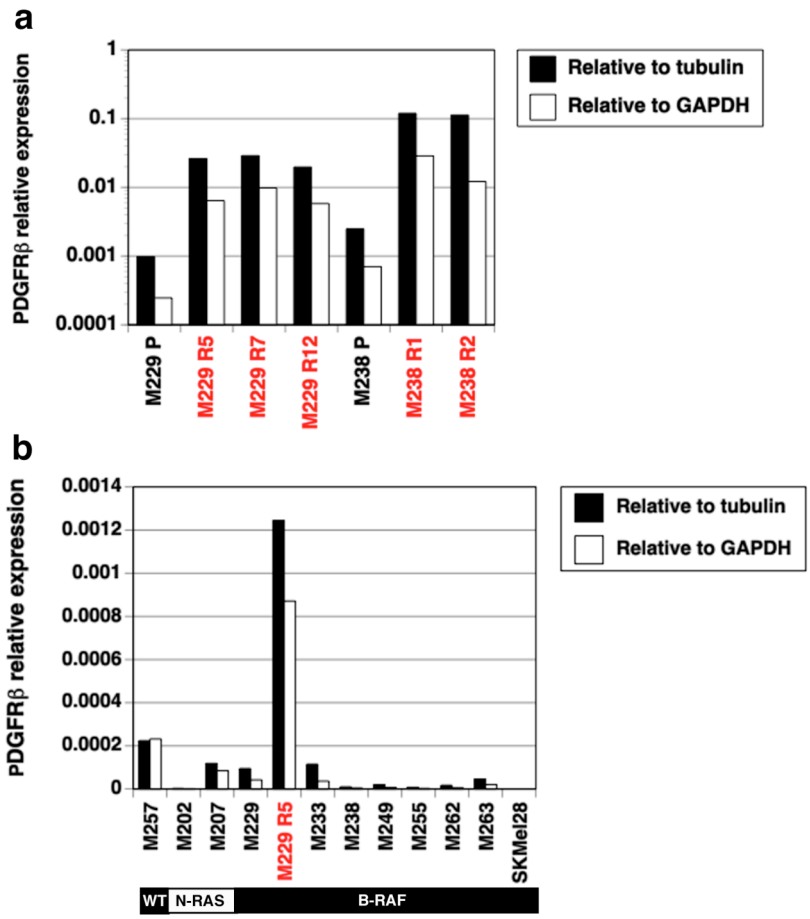

Suppl. Figure 11. PDGFRβ overexpression is a shared feature of PLX4032-resistant sub-lines but uncommon among human melanoma cell lines. **a,** PDGFRβ RNA levels across multiple PLX4032-resistant sub-lines are at least one order of magnitude higher than that in the corresponding parental melanoma cell lines. **b,** Melanoma cell lines of different genotypes (N-RAS/B-RAF WT, N-RAS mutant, and ^{V600E}B-RAF mutant) express low levels of PDGFRβ relative to the PLX4032-resistant sub-line, M229 R5. RNA levels of PDGFRβ were determined by real-time, quantitative PCR and shown as the average of duplicates.

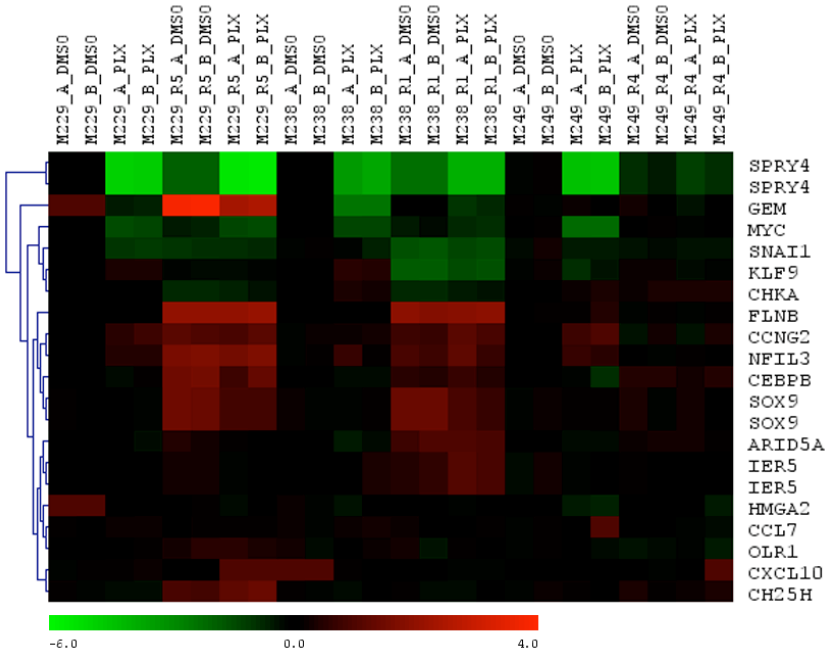

Suppl. Figure 12. PDGFRβ-activated, PLX4032-resistant melanoma sub-lines displayed a PDGFRβ gene signature. Unsupervised hierarchical clustering of parental cell lines and resistant sub-lines with respect to expression of PDGFRβ-responsive genes showing their co-regulation in M229 R5 and M238 R1 but not M249 R4. The relative expression levels were normalized against each of the DMSO-treated parental cell lines.

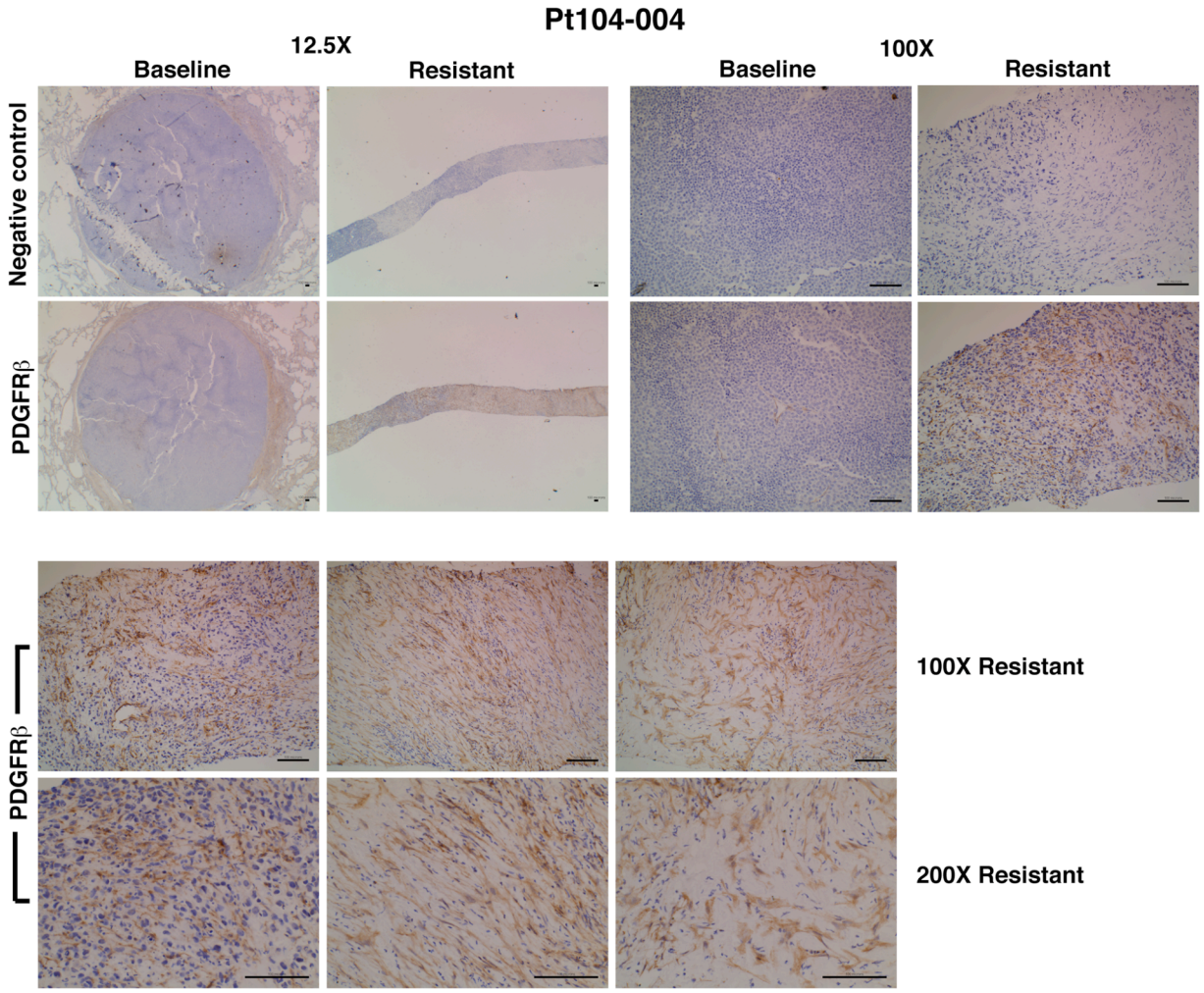

Suppl. Figure 13. PDGFRβ over-expression specifically in melanoma tumor acquiring resistance to PLX4032. An example of immunohistochemistry performed on formalin-fixed, paraffin embedded tissues (paired baseline *vs.* resistant tumors) showing PDGFRβ over-expression in the resistant tumor of a patient (Pt104-004) (top) and additional representative areas of the resistant tumor (bottom). Magnifications shown and black bars, 50 micron.

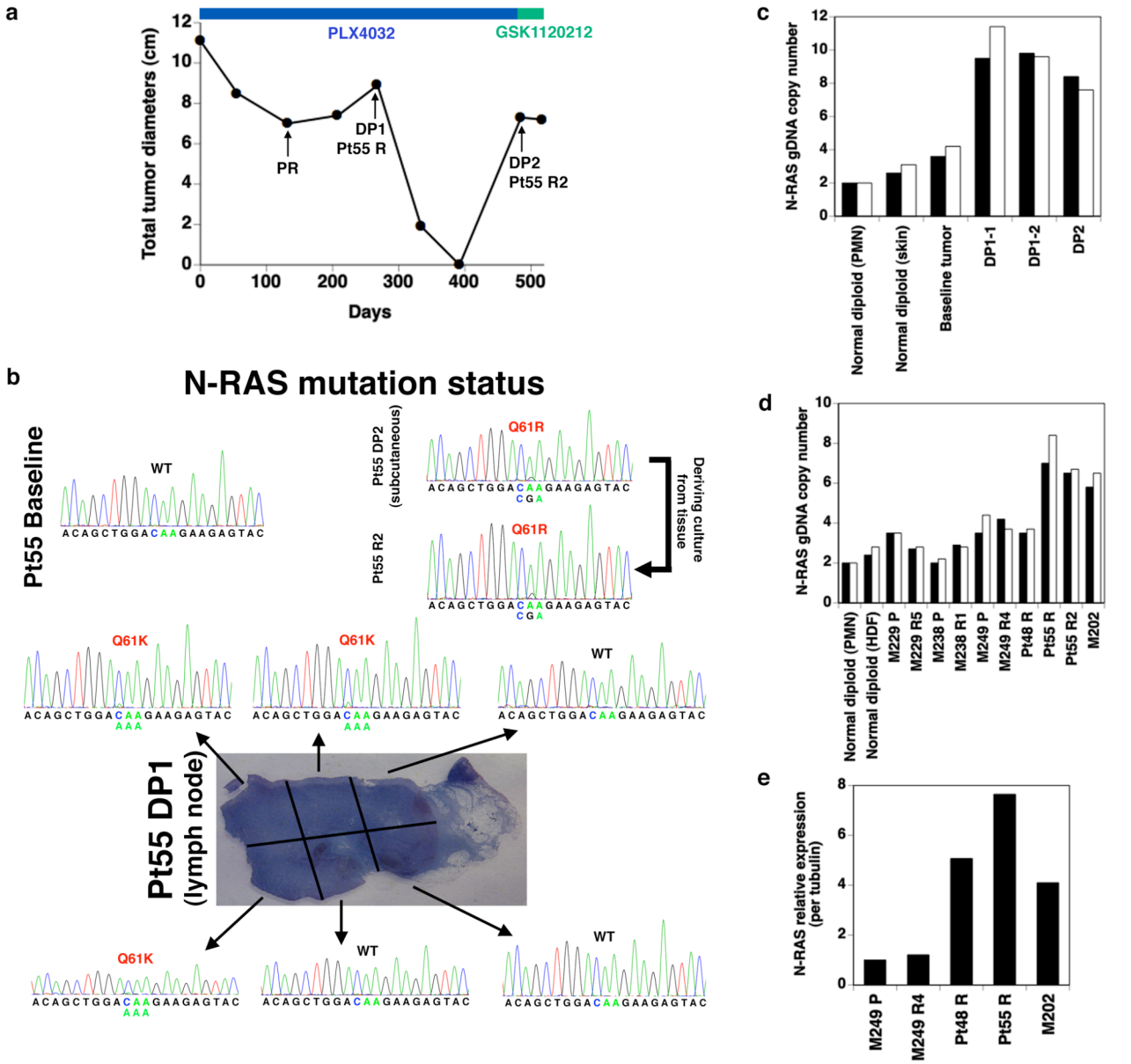

Suppl. Figure 14. *N-RAS* genetic alterations in PLX4032-resistant melanoma tissues and short-term cultures from Pt55 include both mutational activation and gDNA copy gain. **a,** Pt55 tumor tracking (sum of greatest diameters of all target lesions). Arrows indicate times at: partial response (PR), first and second disease progression (DP1 & 2) tumor biopsies (and derived cultures). Nadir at day 400 is attributable to prior surgical intervention. Color bars, oral dosing with PLX4032 and the

MEK inhibitor GSK1120212. **b,** *N-RAS* WT status in Pt55 baseline (pre-treatment) melanoma tissue and mutant status (Q61K in DP1; Q61R in DP2) in PLX4032-resistant melanoma tissues and culture (Q61R in Pt55 R2). The ^{Q61K}*N-RAS* mutation was detectable in three out of six macro-dissected regions in DP1 tissue sections. **c,** *N-RAS* gDNA copy number in Pt55 DP1 (-1 and -2 refer to upper left and upper mid portions of macro-dissected regions in b) and DP2 relative to that in Pt55 baseline tumor, normal, diploid human peripheral mononuclear cells (PMN), and normal skin. Relative gDNA copy numbers were determined by real-time, quantitative PCR, and duplicate data points for each tissue or cell line are displayed (c & d). **d,** *N-RAS* gDNA copy number in Pt55 R relative to that of other indicated cell lines, PMN, and primary neonatal foreskin human dermal fibroblasts (HDF, passage 7). **e,** *N-RAS* RNA overexpression in Pt55 R correlated with its protein overexpression (Fig. 3b). RNA levels of *N-RAS* (relative to tubulin) were determined by real-time, quantitative PCR and shown as the average of duplicates.

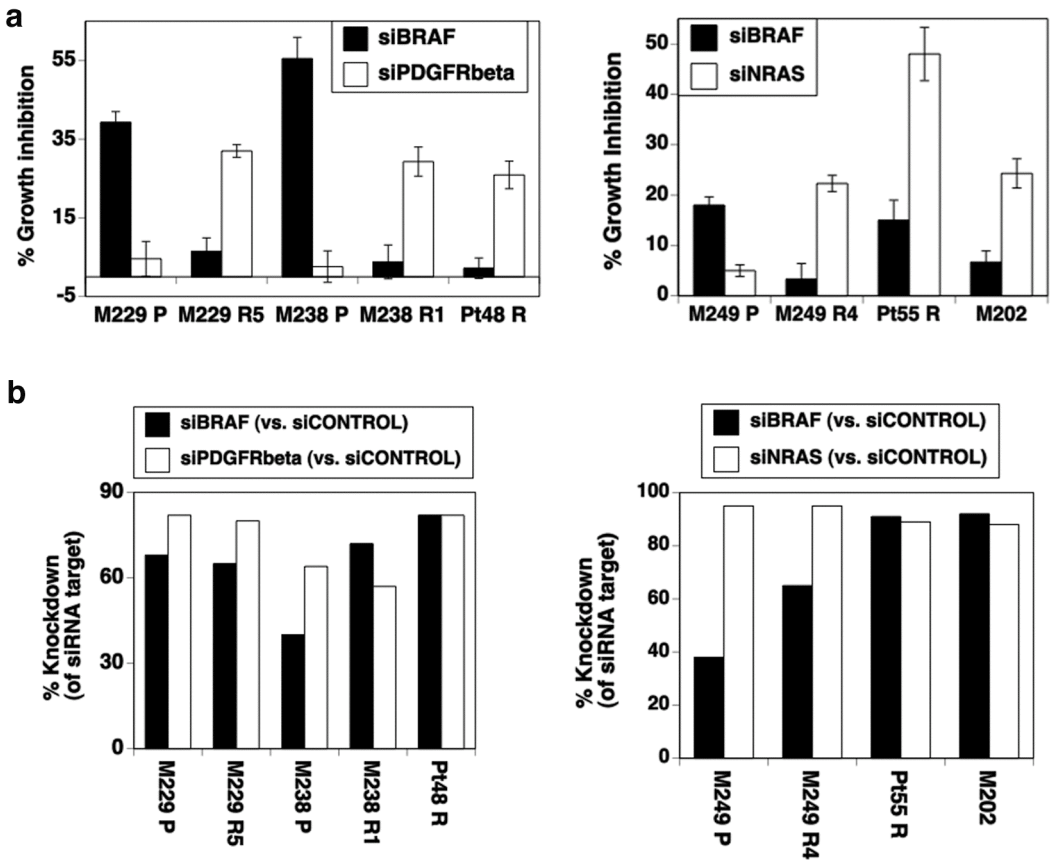

Suppl. Figure 15. Growth of PDGFRβ- or N-RAS-upregulated melanoma cells are preferentially sensitive to gene knockdown by siRNAs. a, Growth-inhibitory effects of siBRAF *vs.* siPDGFRβ or siNRAS (relative to siCONTROL) among PLX4032-sensitive and -resistant melanoma cell lines and cultures (n = 5, mean ± SEM). **b,** B-RAF, PDGFRβ, N-RAS knockdown efficiencies by transient siRNA transfection. RNA levels relative to GAPDH were determined by real-time, quantitative PCR (% KD relative to siCONTROL transfected cells shown as averaged values of duplicates).

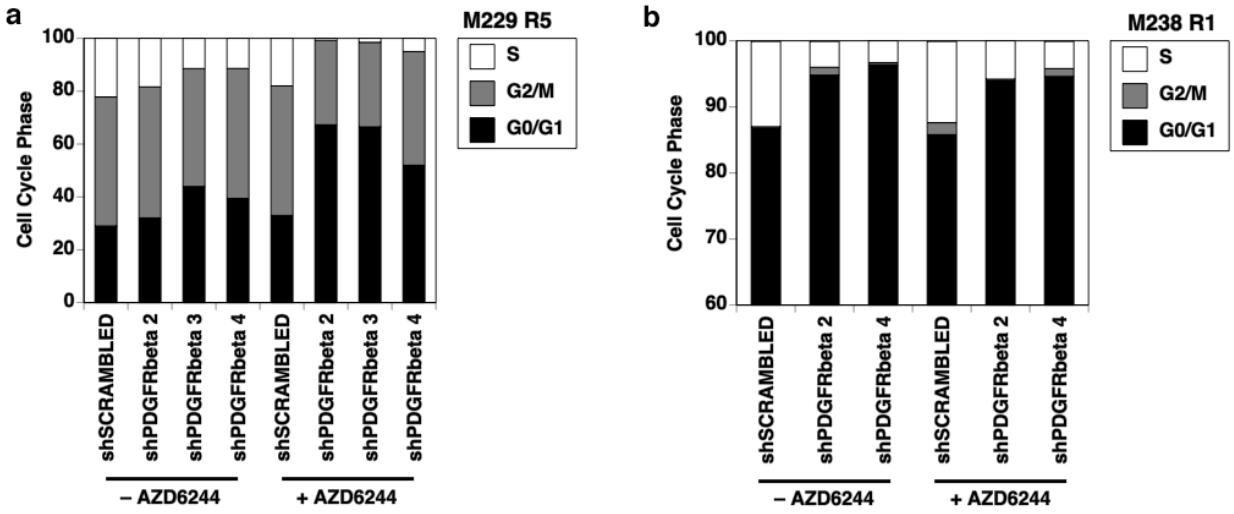

Suppl. Figure 16. PDGFRβ knockdown-induced cell cycle arrest in M229 R5, but not in M238 R1, depends on MEK inhibition. Transduction of individual PDGFRβ shRNAs in M229 R5 (**a**) and M238 R1 (**b**) and their effects on cell cycle distribution.

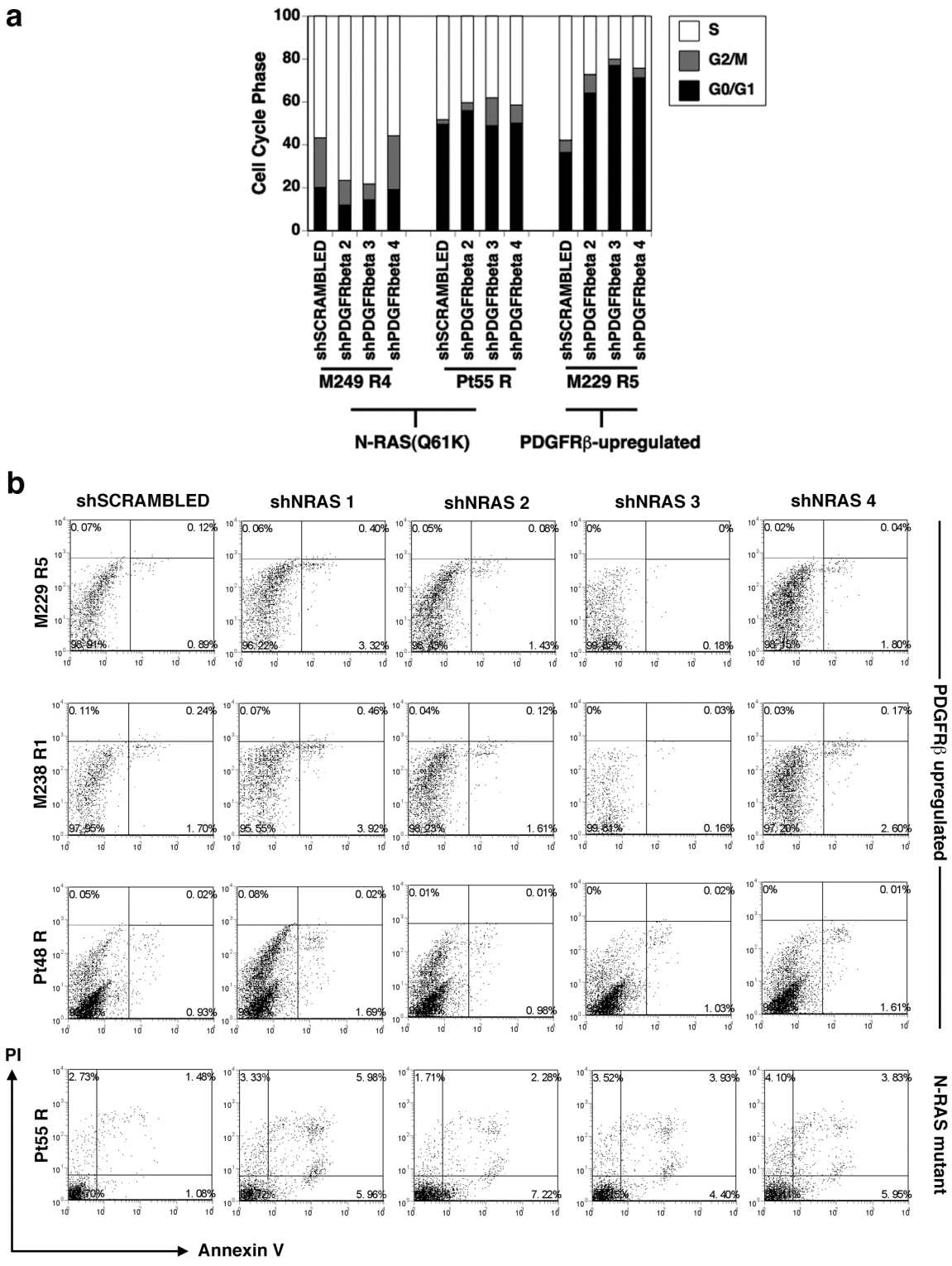

Suppl. Figure 17. Cell cycle arrest and apoptotic responses to PDGFRβ and N-RAS knockdown are specific to PLX4032-resistant cells that respectively over-

express PDGFRβ and harbor mutant N-RAS. a, Transduction of individual PDGFRβ shRNAs in M249 R4, Pt55 R, and M229 R5 (treated with MEK inhibitor AZD6244) and effects on cell cycle distribution (data shown as % of total). **b**, Transduction of individual N-RAS shRNAs in M229 R5, M239 R1, Pt48 R, and Pt55 R and effects on apoptosis. All PLX4032-resistant sub-lines and short-term cultures were incubated with PLX4032 (1 μM) during the experiment; M229 R5 transduced with PDGFRβ shRNAs was co-treated with AZD6244 (0.5 μM).

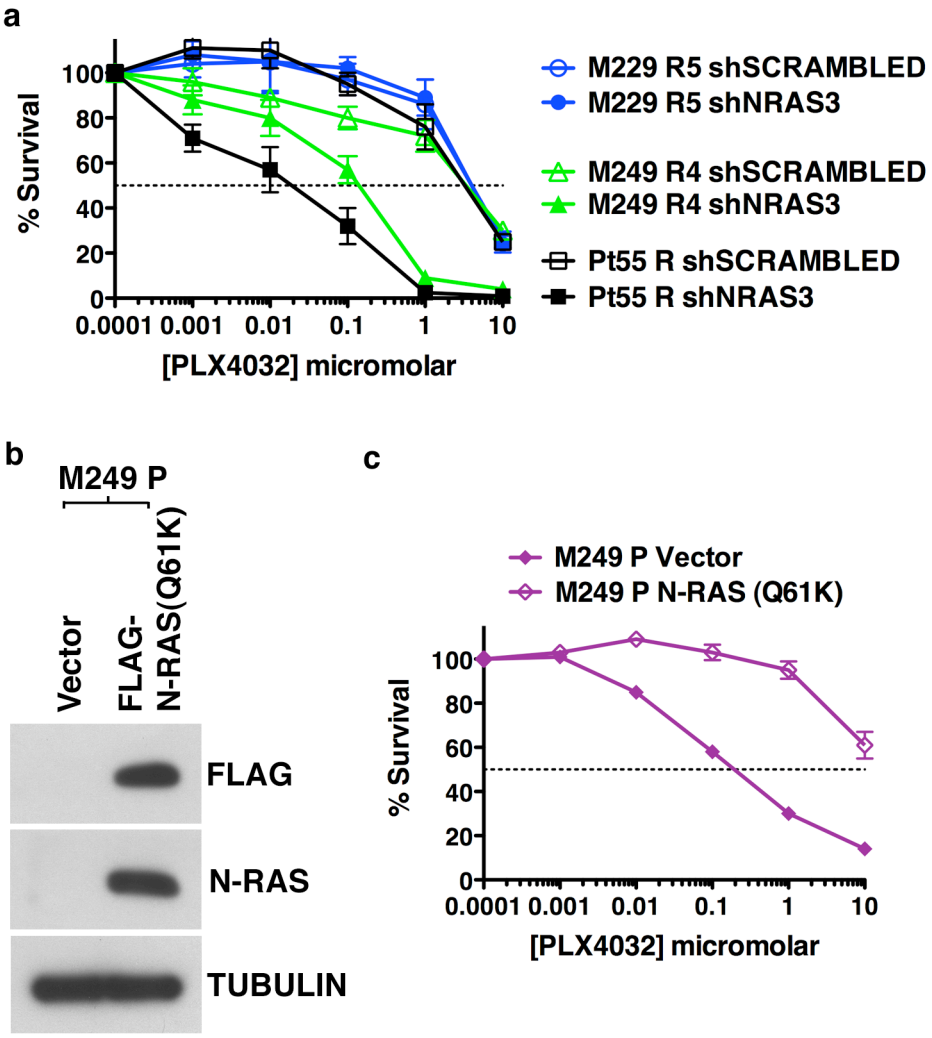

Suppl. Figure 18. Mutant N-RAS levels specifically modulate PLX4032 sensitivity. **a,** Cells were transduced with shSCRAMBLED or shNRAS3 and then treated with the indicated [PLX4032] for 72 h. **b**, Stable over-expression of empty vector *vs*. FLAG-N-RAS(Q61K) in the M249 parental cell line. Lysates were immuno-blotted against FLAG, N-RAS, or TUBULIN (loading control). **c**, Survival curves for cell lines shown in **b** treated with the indicated [PLX4032] for 72 h. Data represent percent surviving cells relative to DMSO-treated controls (mean ± SEM, n = 5). Dashed line, 50% cell killing. Parental line for Pt55 R, not available.

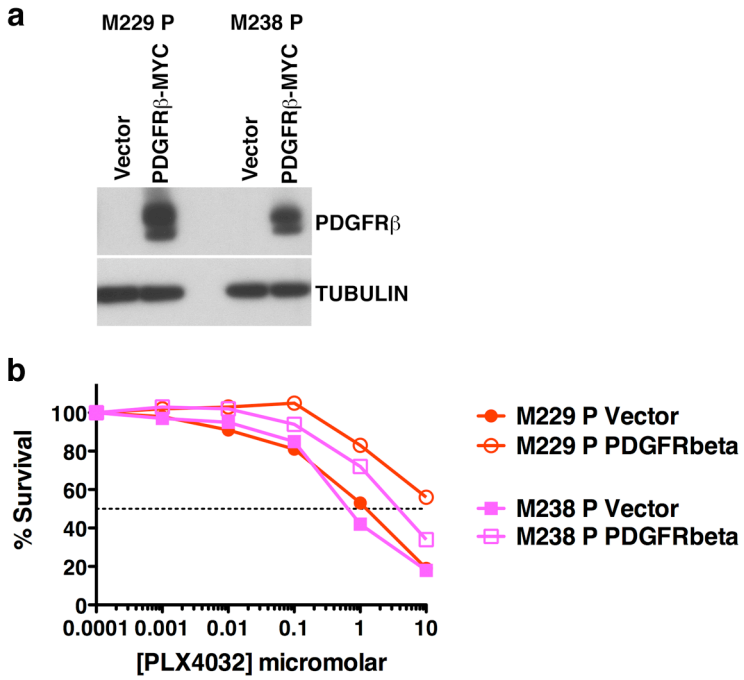

Suppl. Figure 19. PDGFRβ upregulation reduces PLX4032 sensitivity in parental melanoma cell lines. **a**, Stable over-expression of empty vector *vs.* WT PDGFRβ-MYC in the M229 and M238 parental cell lines. Lysates were immuno-blotted against PDGFRβ or TUBULIN (loading control). **b**, Survival curves for cell lines shown in **a** treated with the indicated [PLX4032] for 72 h and PDGF-BB (25 ng/ml) in the over-expression group. Data represent percent surviving cells relative to DMSO-treated controls (mean ± SEM, n = 5). Dashed line, 50% cell killing.

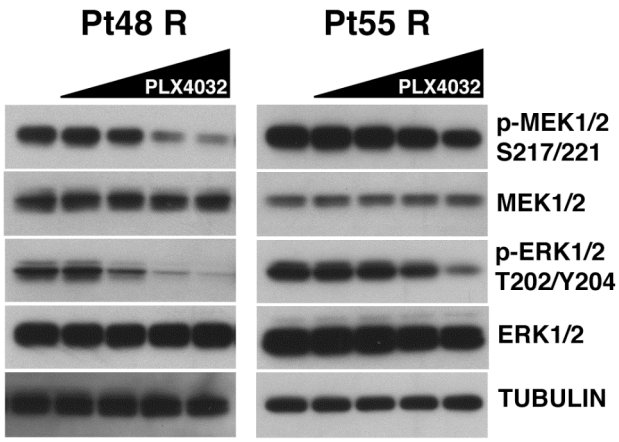

Suppl. Figure 20. Relative MAPK pathway resistance to PLX4032 in Pt55 R relative to Pt48 R. Both PLX4032-resistant cultures were treated with increasing doses of PLX4032 (0, 0.01, 0.1, 1, and 10 μM) and the effects on MAPK signaling were determined by immunoblotting for p-MEK1/2 and p-ERK1/2 levels. Total MEK1/2, ERK1/2 and tubulin levels, loading controls.

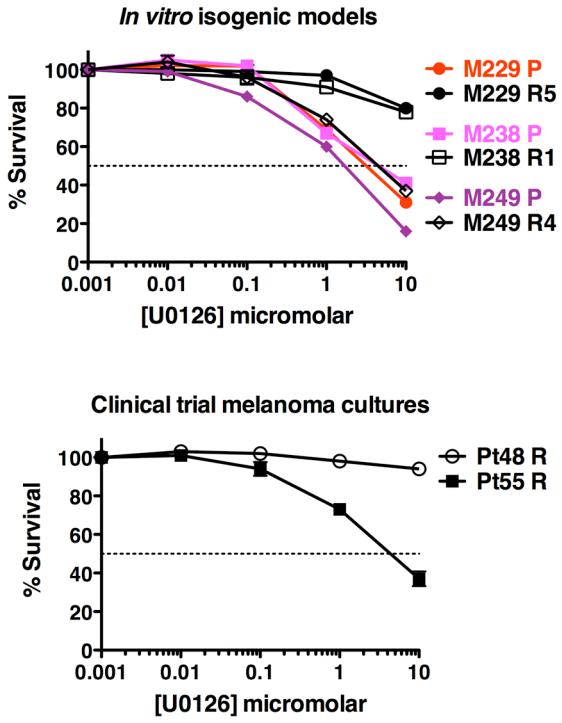

Suppl. Figure 21. PLX4032-resistant, MAPK-reactivated melanoma sub-line (M249 R4) and culture (Pt55 R) display heightened sensitivity to the MEK inhibitor U0126. Cells were treated with the indicated [U0126] for 72 h. Data represent percent surviving cells relative to DMSO-treated controls (mean ± SEM, n = 5). PLX4032-resistant cells were cultured in the presence of PLX4032. Dashed line, 50% cell killing.

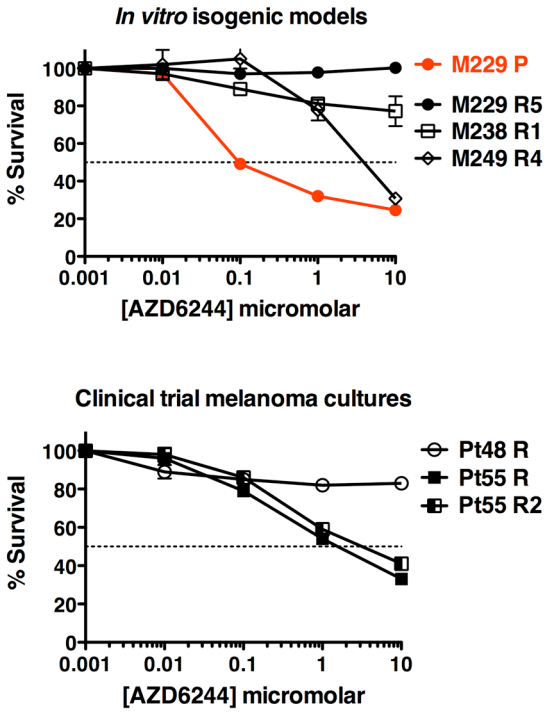

Suppl. Figure 22. Profile of PLX4032-resistant sub-lines and short-term cultures to AZD6244 treatment alone (without PLX4032). AZD6244 selectively growth inhibits N-RAS mutant, PLX4032-resistant melanoma sub-lines (M249 R4) or short-term cultures (Pt55 R, Pt55 R2). PDGFRβ-overexpressing, PLX4032-resistant sub-lines (M229 R5, M238 R1) or cultures (Pt48 R) are cross-resistant to AZD6244. M229 parental (P) cell line was included for reference. Cells were plated in the absence of PLX4032 and treated with the indicated [AZD6244] for 72 h. Data represent percent surviving cells relative to DMSO-treated controls (mean ± SEM, n = 5). Dashed line, 50% cell killing.

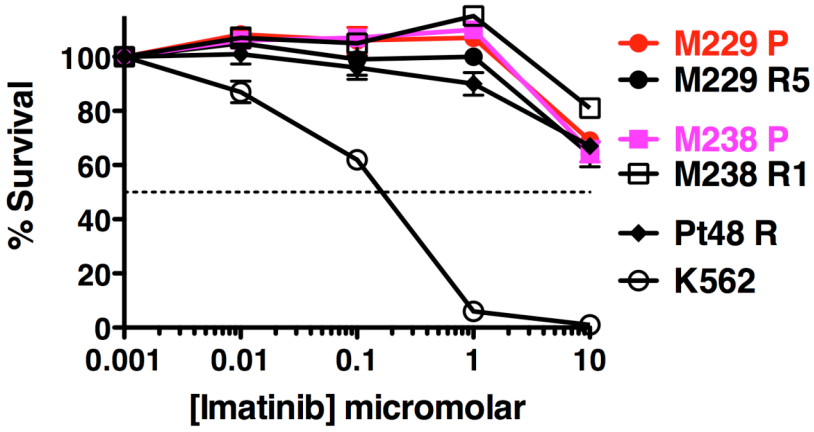

Suppl. Figure 23. PDGFRβ-upregulated, PLX4032-resistant cell lines and culture are highly resistant to imatinib single agent treatment. Survival curves for parental vs. PLX4032-resistant sub-lines and culture in response to imatinib. Cells were treated with the indicated drug concentrations for 72 h in the presence of PLX4032 (1 μM). K562, an imatinib-responsive leukemic cell line, is included as a positive control. Data represent surviving cells relative to DMSO-treated controls (mean ± SD, n=5). The dashed line corresponds to 50% cell killing.